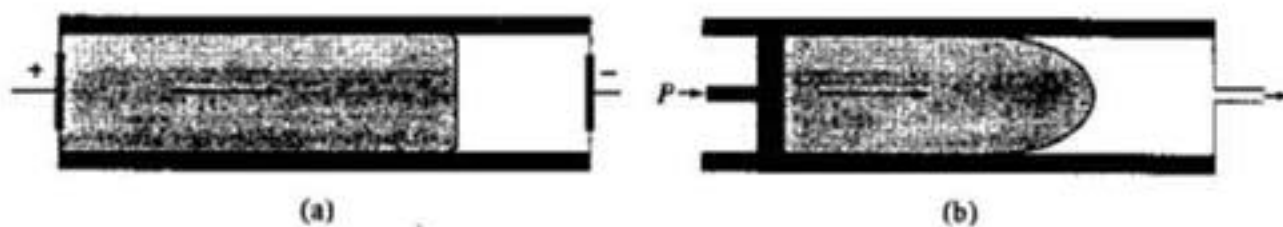
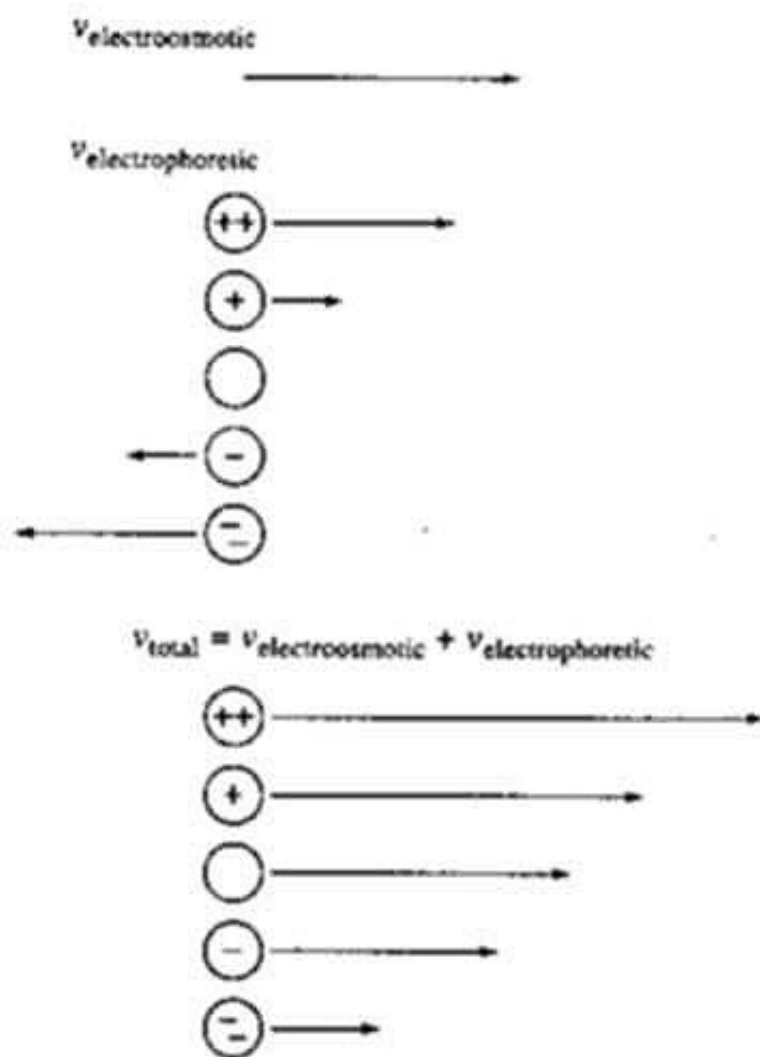


**Figure 30-2** Charge distribution at a silica/capillary interface and resulting electroosmotic flow. (From A. G. Ewing, R. A. Wallingford, and T. M. Olefirowicz, *Anal. Chem.*, 1989, 61, 294A. With permission.)



**Figure 30-3** Flow profiles for liquids under (a) electroosmotic pressure and (b) hydrodynamic pressure.



**Figure 30-4** Velocities in the presence of electroosmotic flow. The length of the arrow next to an ion indicates the magnitude of its velocity; the direction of the arrow indicates the direction of motion. The negative electrode would be to the right, and the positive electrode to the left of this section of solution.

**TABLE 30-1** Detection Modes Developed for Capillary Electrophoresis<sup>a</sup>

Detection Principle	Representative Detection Limit <sup>b</sup> (moles detected)
Spectrometry	
Absorption <sup>c</sup>	$10^{-15}$ – $10^{-13}$
Fluorescence	
Precolumn derivatization	$10^{-17}$ – $10^{-20}$
On-column derivatization	$8 \times 10^{-16}$
Postcolumn derivatization	$2 \times 10^{-17}$
Indirect fluorescence	$5 \times 10^{-17}$
Thermal lens <sup>c</sup>	$4 \times 10^{-17}$
Raman <sup>c</sup>	$2 \times 10^{-15}$
Mass spectrometry	$1 \times 10^{-17}$
Electrochemical	
Conductivity <sup>c</sup>	$1 \times 10^{-16}$
Potentiometry	Not reported
Amperometry	$7 \times 10^{-19}$
Radiometry <sup>c</sup>	$1 \times 10^{-19}$

<sup>a</sup>From A. G. Ewing, R. A. Wallingford, and T. M. Olefirowicz, *Anal. Chem.*, 1989, 61, 298A. With permission.

<sup>b</sup>Detection limits quoted have been determined with a wide variety of injection volumes that range from 18  $\mu$ l to 10  $\mu$ l.

<sup>c</sup>Mass detection limit converted from concentration detection limit using a 1-nL injection volume.

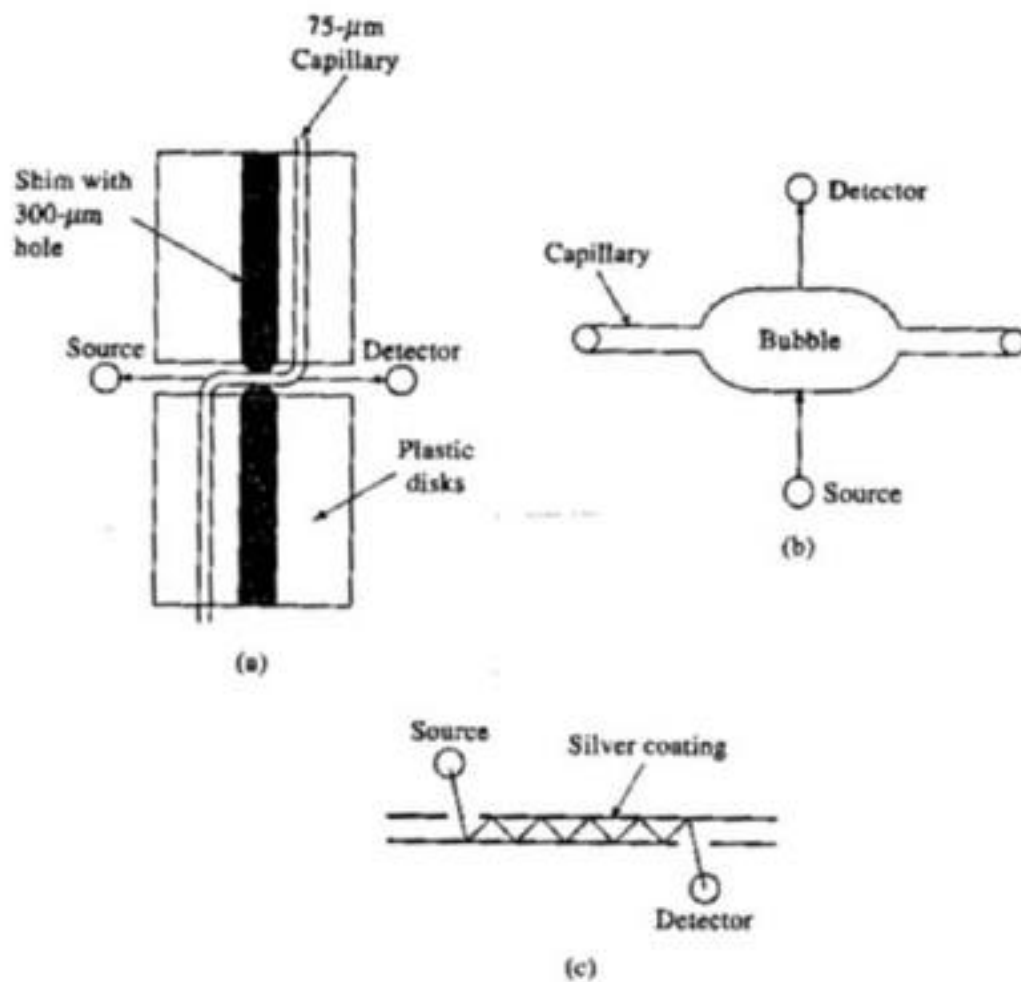


**Figure 30-5** Three types of cells for improving the sensitivity of detection by absorbance measurements: (a) the 3-mm z cell, (b) the 150- $\mu\text{m}$  bubble cell, (c) the multireflection cell.

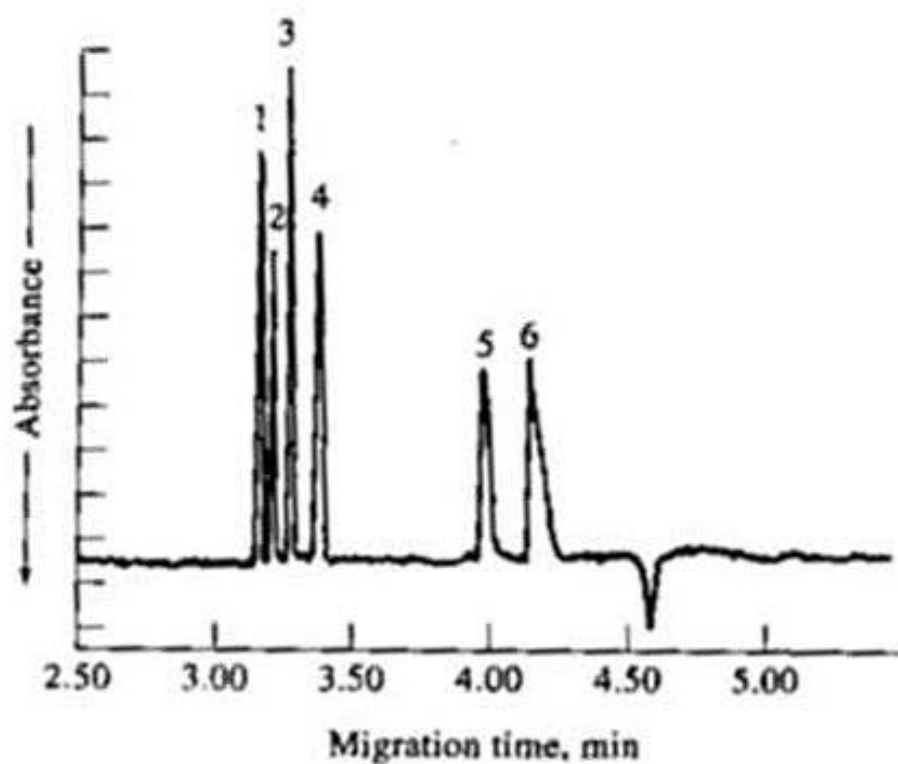


**Figure 30-6** Electropherogram of a six-anion mixture by indirect detection with 4-nM chromate ion at 254 nm. Peak: (1) bromide (4 ppm), (2) chloride (2 ppm), (3) sulfate (4 ppm), (4) nitrate (4 ppm), (5) fluoride (1 ppm), (6) phosphate (6 ppm).

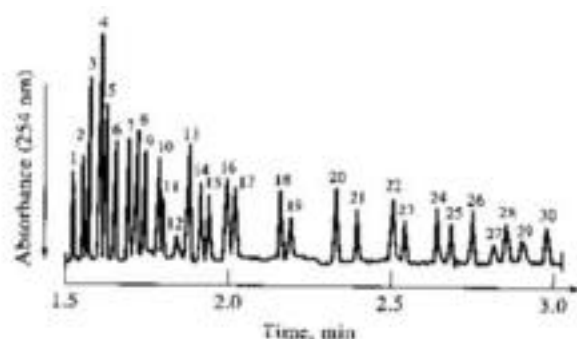


**Figure 30-10** Electropherogram showing the separation of 30 anions. Capillary internal diameter: 50  $\mu\text{m}$  (fused silica). Detection: indirect UV, 254 nm. Peaks: 1 = thiosulfate (4 ppm), 2 = bromide (4 ppm), 3 = chloride (2 ppm), 4 = sulfate (4 ppm), 5 = nitrite (4 ppm), 6 = nitrate (4 ppm), 7 = molybdate (10 ppm), 8 = azide (4 ppm), 9 = tungstate (10 ppm), 10 = monofluorophosphate (5 ppm), 11 = chlorate (4 ppm), 12 = citrate (2 ppm), 13 = fluoride (1 ppm), 14 = formate (2 ppm), 15 = phosphate (4 ppm), 16 = phosphite (4 ppm), 17 = chlorite (4 ppm), 18 = galactarate (5 ppm), 19 = carbonate (4 ppm), 20 = acetate (4 ppm), 21 = ethanesulfonate (4 ppm), 22 = propionate (5 ppm), 23 = propanesulfonate (4 ppm), 24 = butyrate (5 ppm), 25 = butanesulfonate (4 ppm), 26 = valerate (5 ppm), 27 = benzoate (4 ppm), 28 = *l*-glutamate (5 ppm), 29 = pentanesulfonate (4 ppm), 30 = *d*-gluconate (5 ppm). (From W. A. Jones and P. Jandik, *J. Chromatogr.*, 1991, 546, 445. With permission.)

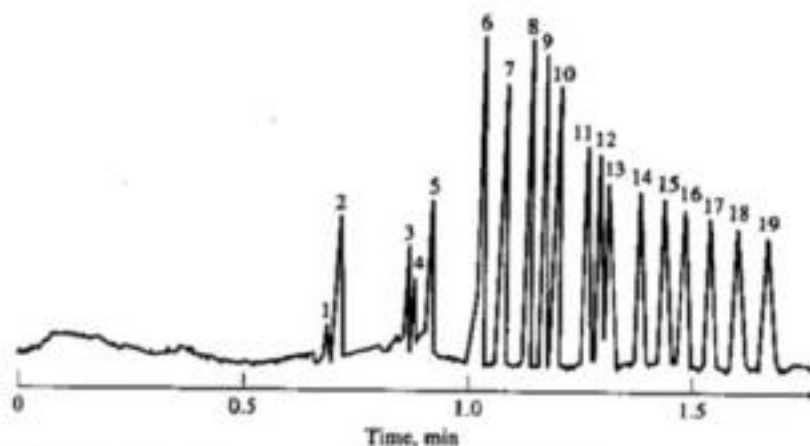


**Figure 30-11** Separation of alkali, alkaline earths, and lanthanides. Capillary: 36.5 cm  $\times$  75- $\mu\text{m}$  fused silica, +30 kV. Injection: hydrostatic, 20 s at 10 cm. Detection: indirect UV, 214 nm. Peaks: 1 = rubidium (2 ppm), 2 = potassium (5 ppm), 3 = calcium (2 ppm), 4 = sodium (1 ppm), 5 = magnesium (1 ppm), 6 = lithium (1 ppm), 7 = lanthanum (5 ppm), 8 = cerium (5 ppm), 9 = praseodymium (5 ppm), 10 = neodymium (5 ppm), 11 = samarium (5 ppm), 12 = europium (5 ppm), 13 = gadolinium (5 ppm), 14 = terbium (5 ppm), 15 = dysprosium (5 ppm), 16 = holmium (5 ppm), 17 = erbium (5 ppm), 18 = thulium (5 ppm), 19 = ytterbium (5 ppm). (From P. Jandik, W. R. Jones, O. Weston, and P. R. Brown, *LC-GC*, 1991, 9, 634. With permission.)